*Clinical Neurophysiology*

# A NEW METHOD FOR THE ESTIMATION OF MOTOR NERVE CONDUCTION BLOCK

**Luca Mesin[1], Dario Cocito[2,3].**

[1] *LISiN, Dip. di Elettronica, Politecnico di Torino, Torino, Italy*

[2] *S.C. Neurologia con indirizzo di Riabilitazione Funzionale, Dipartimento di Neuroscienze, Università di Torino, Torino, Italy*
[3] *Divisione di Riabilitazione Neuromotoria, Casa di Cura Major di Torino, I.R.C.C.S. Fondazione S. Maugeri, Pavia, Italy*

**Keywords:** CMAP, EMG signal, motor response, conduction block.

**Running title:** Estimation of motor nerve conduction block

## Address for correspondence:

Luca Mesin, Ph.D.

Dipartimento di Elettronica, Politecnico di Torino; Corso Duca degli Abruzzi 24, Torino, 10129 ITALY

Tel. 0039-011-4330476; Fax. 0039-0114330404; e-mail : luca.mesin@eln.polito.it

## Acknowledgements

This study was supported by project A76 " Manifestazioni mioelettriche di fatica muscolare in neuropatie demielinizzanti:caratterizzazione e impatto della terapia" sponsored by Regione Piemonte, Italy.

**ABSTRACT**

**Objective:** A method for conduction block (CB) estimation, based on compound muscle action potentials (CMAP) elicited by stimulation at sites proximal and distal to the region in which a block is suspected, which is less sensitive to temporal dispersion than methods based on area and amplitude estimation, routinely used in clinical practice.

**Methods:** The method is based on deconvolution of CMAPs. It provides the delay distribution that convolved with a kernel (estimated by an optimisation method) gives a reconstruction of the CMAPs. The integral of the delay distribution was used to estimate CB. The method was tested on phenomenological signals (sum of delayed and amplitude scaled versions of the same signal), structure based simulated signals (from a plane layer generation model of surface EMG), and experimental signals (8 healthy subjects; CMAPs recorded over abductor digiti minimi; different temporal dispersions obtained comparing above-elbow stimulation of ulnar nerve with below–elbow stimulation or with wrist stimulation - conduction distances about 10 and 35 cm, respectively).

**Results:** Deconvolution method gives more precise estimates of the simulated CB with respect to area and amplitude methods (phenomenological signals: bias in CB estimation in the worst case about 10% for deconvolution, 30% for area, 60% for amplitude). Experimental data: by increasing temporal dispersion, in the average CB estimation increases 4% for area and 10% for amplitude, no increase for deconvolution.

**Conclusions:** The new method for CB estimation is less sensitive to temporal dispersion than area and amplitude methods.

**Significance:** The proposed method provides a precise CB estimation. Being stable to temporal dispersion, it allows to diagnose CB with a lower confidence threshold than in the case of area and amplitude.

## 1. INTRODUCTION

Conduction block (CB) is defined as a block of impulse transmission in nerve fibres whose axons are intact. Patients affected by CB show muscle weakness.

There are several possible mechanisms inducing CB, but most are related to the demyelination of the axons (Feasby et al., 1985; Kimura, 1993). The lesion of the myelin sheaths determines the block of impulses or an abnormal temporal dispersion of the action potential propagation along the nerve (Schulte-Mattler et al., 1999). CB may also occur in the case of axons damage. Both CB and temporal dispersion may result in a reduced area and amplitude of the compound muscle action potential (CMAP). Furthermore, temporal dispersion in motor nerves is also associated with changes of duration and Fourier spectra of the CMAP. It was proved on experimental signals that these changes depend on the length of the nerve segment (Schulte-Mattler et al., 2001).

Different criteria were proposed for the estimation of CB. Most of them rely on comparing the CMAP following stimulation at a proximal and at a distal site. The parameters usually extracted from such two CMAPs are the area and the amplitude, which are then used to estimate CB in clinical applications.

Estimating CB on the recorded CMAPs is an inverse problem (Tikhonov and Arsenin, 1977; Schoonhoven and Stegeman, 1991). No a priori information on the effective CB in a patient is available in order to validate a method. Furthermore, experimental data are affected by noise, by muscle crosstalk, and by the actual capability of stimulating exactly the same axons at the two stimulation sites. For this reasons, the validation of a method should be based on simulations, which can assess the accuracy of the CB estimation and the conditions of validity of a method. The effect of both CB and temporal dispersion on the detected CMAP was addressed in many simulation studies (Rhee et al., 1990; Tani et al., 1997; Stalberg and Karlsson, 2001; Reutskiy et al., 2003). CB estimated considering the area and the amplitude

was compared to the simulated CB. As abnormal temporal dispersion can strongly affect both parameters (Rhee et al., 1990), it was suggested to diagnose a CB only when the decrease in area and amplitude is bigger than a high confidence threshold ($\geq$50% Rhee et al., 1990). Some works suggested to study both the area or amplitude decrease and the temporal dispersion (estimated by the negative-peak duration method, Oh et al., 1994). The American Academy of Neurophysiology, 1991, proposed as a criteria for CB a more than 20% drop in the area or peak-to-peak amplitude (distal versus proximal CMAP) with less than a 15% change in the duration. A recent paper (Asseldonk et al., 2006) proposed different confidence thresholds as a function of the estimated duration prolongation on proximal versus distal stimulation; more flexible sets of criteria for forearm segments are provided in the case of large temporal dispersion.

In this paper we introduce a new method for the estimation of CB, based on the deconvolution of the CMAPs. The method provides the delay distribution that convolved with a kernel gives an approximate reconstruction of the CMAPs. The kernel is estimated by an optimisation procedure which minimises the error in the reconstruction of the data (distal and proximal CMAPs) as the convolution of the kernel with the estimated delay distributions. The integral of the delay distribution was considered as an estimate of the number of active motor units (MU), and was used to estimate CB. As the contribution of different MUs depends on their dimension and location, the estimate of the number of active MUs (and therefore also the estimate of CB) is only approximated. Nevertheless, area and amplitude are also affected by the dimension and location of the elicited MUs. The advantage of deconvolution over methods based on area and amplitude is that of being (ideally) insensitive to temporal dispersion.

The method was applied to both phenomenological, simulated and experimental signals and proved to be stable to temporal dispersion.

## 2. METHODS

### 2.1 Mathematical model and notations

A CMAP is the sum of the action potentials generated by the MUs activated by a stimulating current:

$$v(t) = \sum_{n=1}^{N} v_n(t - \tau_n) \tag{1}$$

where $v(t)$ is the CMAP, $N$ the number of the elicited MUs, $v_n(t)$ the action potential corresponding to the n$^{th}$ MU, $\tau_n$ its delay. The delay $\tau_n$ of the n$^{th}$ MUAP $v_n(t)$ corresponds to the time of propagation of the action potential along the nerve. The delay distribution depends on the nerve conduction velocity (CVN) distribution.

An impulse, which travelled along a motor axon and arrived at the end-plate, primes the generation of the transmembrane current transient, which travels from the end-plate to the tendon endings and induces fibre contraction. The time delay at the neuro-muscular junction will be neglected (which corresponds to the assumption that the time delays are constant for each junction). The n$^{th}$ MUAP shape $v_n(t)$ depends on the location of the fibres constituting the MU, on the geometry and conductivity of the physiological tissues (referred to as volume conductor) and on the conduction velocity (CVM) of such fibres (introducing a temporal scaling factor). CVM is about the same for all the fibres constituting the same MU, but differs between different MUs. Normal values are between 3 and 5 m/s (Troni et al., 1983).

The determination of the distribution of delays implies the estimation of $N$, $\tau_n$ and action potential shapes $v_n(t)$, given the recorded CMAP $v(t)$. This problem is under determined, thus some assumptions are needed to reduce the number of unknowns. We will assume that all action potentials $v_n(t)$ have the same shape and differ only for the amplitude:

$$v(t) \cong \sum_{n=1}^{N} A_n K(t - \tau_n). \quad (2)$$

The function $K(t)$, defining the shape of the action potentials, will be referred to as the *kernel*. Model (2) requires that the MUAPs are quite similar in shape, which is a strong approximation, as a MUAP shape (as stated above) depends on the location of the MU, on the volume conductor, on the dispersion of the end-plates and on CVM. Skipping the approximation sign, Eq. (2) can be rewritten as (Schoonhoven and Stegeman, 1991):

$$v(t) = K(t) * x(t) \quad (3)$$

where the symbol * indicates convolution, and the function $x(t)$ defines the delay distribution (see Figure 1A for a sketchy representation of convolution).

As the MUs are not innervated exactly in the same point, the delay $\tau_n$ is affected by the different propagation length along the muscle fibres. This means that in model (2) both the time delay due to the propagation of the action potential along the axon and the time delay due to the propagation of the action potential along the muscle fibres are considered. Furthermore, MUs with different CVM give MUAPs which appear approximately as versions of a waveform (which can be approximated by $K(t)$) scaled in time. The scaling effect is not modelled by (2). Nevertheless a scaled version $v_1(t)$ of function $K(t)$ can be rebuilt by the convolution of $K(t)$ with a delay distribution function $x_1(t)$ (determining a diffusion effect on the kernel $K(t)$). This is another contribution to the delay distribution given by the propagation of the action potentials along the muscle fibres.

For noisy recordings, a white noise *n(t)* can be added:

$$v(t) = K(t) * x(t) + n(t) \quad (4)$$

## 2.2 CB estimation

CB is estimated from the delay distributions of the MUAPs contributing to the distal and proximal CMAPs, indicated by $x^{dist}(t)$ and $x^{prox}(t)$, respectively. The suggested estimation of CB is the following:

$$CB = 1 - \frac{\int x^{prox}(t)dt}{\int x^{dist}(t)dt}. \quad (5)$$

The estimation of CB by Eq. (5) requires the solution of Eq. (3), i.e. the inversion of a convolution equation, referred to as *deconvolution*. The method to estimate both the kernel and the delay distribution by deconvolution (i.e., a blind deconvolution) is described in the Appendix.

## 2.3 EMG signals simulation

Both phenomenological signals and simulated signals were used to compare the new method to classical methods based on area and amplitude.

### *2.3.1 Phenomenological signals*

Phenomenological signals were generated by summing delayed versions of the same waveform scaled in amplitude.

The same method discussed in Rhee et al., 1990, was used, but the representative MUAP was estimated averaging signals recorded from a human muscle instead of averaging signals from mouse muscles. The signals acquired within the work Mesin et al., 2006, were used to obtain the representative MUAP. Experimental monopolar surface EMG signals were collected from the abductor pollicis brevis muscle of 8 subjects by a linear array of 16 electrodes (inter-electrode distance 2.5 mm, electrodes 1 mm diameter), located between the most distal tendon and the muscle belly, along the direction of the muscle fibres. From the monopolar signals, bipolar derivations were obtained off-line and decomposed to identify

single MUAPs with the method described in Gazzoni et al., 2004 (see also Asseldonk et al., 2006, for another example of simulation study based on single MUAPs extracted from abductor pollicis brevis by spike triggered averaging technique). Ten single MUAPs were obtained by decomposing the interference surface EMG signals. The representative MUAP was defined as the average of these single MUAPs. The result is shown in Figure 2A. Conduction velocity distribution was selected as in Rhee et al., 1990 (see Figure 2B). It is worth noticing that such a distribution of conduction velocity, chosen by Rhee et al., 1990, in the physiologic range of sural nerve of mice (from 28 to 55 m/s), is also close to the physiologic range for normal human median nerve (which is in the range from 35 to 60 m/s), innervating abductor pollicis muscle. The amplitudes of the MUs were distributed as an exponential function (Enoka and Fuglevand, 2001),

$$y_i = ae^{\frac{\ln R}{n} i} \tag{6}$$

where $y_i$ is the innervation number of the i$^{th}$ unit, $a$ is the innervation number (arbitrarily chosen equal to 1, as it does not affect CB estimation), $n$ is the number of MUs (chosen equal to 60, as in Rhee et al., 1990) and R is the ratio of the innervation numbers $R = y_n / y_1$.

Three values for the ratio R were studied, to simulate amplitude ranges of 1, 10, 150, respectively (as in Rhee et al., 1990). An increase of temporal dispersion was simulated by increasing the distance between proximal and distal stimulation sites. As in Rhee et al., 1990, the distal stimulation site was at 10 mm from the motor point, whereas the proximal stimulation site was varied in the range from 10 mm to 500 mm.

*2.3.2 Simulated signals*

A Gaussian CVN distribution centred at 47.3 m/s and with standard deviation 5.2 m/s was simulated. Possible simulated CVN values lower than 35 m/s or higher than 60 m/s were excluded.

The three plane layer model (skin, fat, muscle) proposed by Farina and Merletti, 2001, was used to simulate surface EMG signals. The skin and fat layers were isotropic (skin conductivity 1 S/m; fat conductivity 0.05 S/m), the muscle layer was anisotropic (transversal conductivity 0.1 S/m, longitudinal conductivity 0.5 S/m), with larger conductivity in the direction of the fibres. The detection electrodes were circular, with diameter 10 mm, in single differential configuration, with belly-tendon recording (Kimura, 1989). The source is represented as a spatio-temporal function (analytical model from Rosenfalck, 1969) which describes generation, propagation, and extinction of the intra-cellular action potential at the end-plate, along the fibre, and at the tendons, respectively. The model is shown in Figure 1B. A library of 210 single fibre action potentials (SFAP - in uniform positions within the muscle) was simulated.

The number of fibres in the MUs were distributed as an exponential function (6). The ratio of innervation number was 50. Different subjects were simulated by choosing randomly the positions of the MUs. The end-plates and tendon endings in the MU had a spread of 10 mm. To reduce computational time, all the fibres in a MU were considered concentrated in the same point which was assumed as the centre of the MU territory. The summed contributions were asynchronised due to the spread of end-plates and tendons.

CVM distribution was chosen in the range 3-5 m/s, assuming higher CVM values for larger MUs. Different CVM were simulated by scaling in time the correspondent prototype MUAP (simulated for CVM = 4 m/s). It was assumed that fast axons innervate fast MUs. A linear relation between CVN and CVM was used.

Each simulated signal was obtained adding 210 MUAPs. The activation of the MUs were delayed by the time needed for the action potential to propagate from the stimulation site to the end-plate. To simulate a maximal stimulation, all the 210 MUAPs were added for CMAP

related to the distal stimulation site; to simulate CB, only a percentage of randomly chosen MUAPs were added to simulate the CMAP related to the proximal stimulation site.

A white noise with 20 dB SNR (signal to noise ratio) was added to the obtained CMAP.

*2.3.3 Experimental signals*

Eight male healthy subjects (age, mean ± SD, 28± 5 years; stature, 179 ± 7 cm; weight, 72 ± 4 kg) participated to the measurements. All subjects gave their informed consent, and the study was approved by the local ethics committee.

Surface EMG signals were recorded from the right (dominant) abductor digiti minimi muscle, after stimulation of the ulnar nerve above-elbow (proximal site) and below-elbow or wrist (distal site). The experimental protocol was as in Olney et al., 1987, where the effect of temporal dispersion on area estimates was studied. The distances from the motor point to the wrist, to below-elbow, to above-elbow were 78.5 ± 3.7 mm, 325.4 ± 18.4 mm, 424.2 ± 17.4 mm (mean ± SD), respectively.

Standard procedures for ulnar nerve stimulation were applied (adhesive surface electrodes, with diameter 10 mm, placed over the abductor digiti minimi muscle; single differential configuration, with belly-tendon recording as described in Kimura, 1989; stimulation by a bi-phasic, square, 0.1 ms long, supra-maximal stimulus, from a Viking Select device [Nicolet Biomedical Inc. Madison, WI USA]; responses filtered between 2 Hz and 10 kHz; skin temperature maintained above 35°C).

## 3. RESULTS

The proposed method was applied to phenomenological, simulated and experimental signals.

### 3.1 Results on the simulation of phenomenological signals

The representative MUAP is shown in Figure 2A. The CVN distribution for the phenomenological signals is shown in Figure 2B. The proposed method based on deconvolution (Figure 2C) is compared to classical methods for CB estimation based on measures of area (Figure 2D) and amplitude (Figure 2E), in the case of increasing temporal dispersion induced by an increasing distance from proximal to distal stimulation sites. As phenomenological signals match the hypotheses under which deconvolution method works properly (i.e., all simulated MUAPs constituting the CMAPs have the same shape and no noise was added), no limitation on CVN was needed to be imposed to improve the performance of the method (i.e., $CVN_{\min} = 0,\ \ CVN_{\max} = +\infty$, see the Appendix). As noted in Rhee et al., 1990, both methods based on area and amplitude estimations are more and more biased as temporal dispersion increases. Deconvolution is less sensitive to temporal dispersion. The results of this simulation are in line with Rhee et al., 1990, but with a lower effect of phase cancellation, due to the longer temporal support of the representative MUAP.

### 3.2 Results on signals simulated by a structure based model

CB estimations from signals simulated by a structure based generation model of surface EMG are shown in Figure 3. Delay distributions were constrained considering $CVN_{\min} = 30\ m/s,\ \ CVN_{\max} = 65\ m/s$. The blocked fibres were selected randomly among the simulated fibres. The conduction distance (i.e., the distance between the proximal and the distal stimulation sites) was 250 mm. An example of simulated and reconstructed distal and proximal CMAPs, optimal estimated kernel and estimated delay distributions are shown in Figure 3A. The proposed method based on deconvolution is compared to the methods based on measures of area and amplitude in Figure 3B, showing the average value and standard deviation of the estimates over 25 realisations (correspondent to five different simulated subjects, i.e. different spatial distribution of the simulated MUs, each with five realisations

of the additive noise; see Section 2.3.2). The proposed method performs better than the other two methods considered, which are positively biased by temporal dispersion.

The effect of temporal dispersion is analysed in Figure 4, for the case of simulated signals from a structure based model. The same parameters as in Figure 3 were used, except for the conduction distance, which was varied in the range 100 – 350 mm. The area and the amplitude increase as the conduction distance increases (and then also temporal dispersion increases). Deconvolution is stable to temporal dispersion.

### 3.3 Results on experimental signals

The application on experimental signals is shown in Figure 5. CB were estimated with deconvolution, area and amplitude methods, comparing stimulation above-elbow with below-elbow and above-elbow with wrist. The distances between stimulation sites were 98.8 ± 3.0 mm and 345.8 ± 15.4 mm, respectively. Such difference determines different temporal dispersion in the signals. Mean and standard deviation of the estimated CB over a set of eight healthy subjects (see Section 2.3.3) are shown in Figure 5. Methods based on area and amplitude indicate (in the average) a larger estimated CB for increasing conduction distance, i.e. when comparing above-elbow with wrist, with respect to the case of comparing above-elbow with below-elbow, showing the sensitivity to temporal dispersion discussed in many papers (Rhee et al., 1990; Olney et al., 1987). Deconvolution method shows independence from temporal dispersion.

## 4. DISCUSSION AND CONCLUSIONS

In this paper we introduced a new method for the estimation of CB, based on the deconvolution of the CMAP. The method was applied to phenomenological, simulated and experimental signals.

### 4.1 Discussion of tests based on simulations

Deconvolution gives more accurate estimation of CB with respect to area and amplitude methods in the simulated conditions. The advantage of deconvolution with respect to area and amplitude methods is that it is not affected (ideally) by MUAP temporal dispersion due to the spread of CVN and CVM.

In the case of phenomenological signals, all the hypotheses of deconvolution method (see Section 2.1) are satisfied. An increasing positive bias in the estimates given by area (maximum bias about 30%) and amplitude (maximum bias about 60%) methods is obtained for increasing temporal dispersion, whereas the bias is lower in the case of deconvolution method (less than 10%) indicating the correct operation of the method in ideal conditions. These results confirm the outcome of Rhee et al., 1990, but with a slightly lower sensitivity of area and amplitude to temporal dispersion. This is probably due to the representative MUAP chosen, which was extracted from human abductor pollicis, instead of mouse sural muscle (considered in Rhee et al., 1990). The considered representative MUAP from human abductor pollicis had a longer duration with respect to that used in Rhee et al., 1990. This can be due to two reasons (in addition to the objective difference in considering a human versus a mouse muscle): 1) the experimental signals we considered to extract a MUAP template were at low contraction levels (in order to allow their decomposition), so that the recruited MUs are those propagating at lower velocity; 2) Rhee et al., 1990, used a subcutaneous placement of the recording electrodes, whereas we considered a surface detection (so that the potentials were low pass filtered by the fat and skin tissues).

More realistic simulations are also considered in this work. Using an advanced generation model of surface EMG signals, the effect of different CVM (determining a scaling in time) and of tissues interposed between the sources and the detection electrodes (which determine

shape variations between different MUAPs) was taken into account. In a representative set of simulations (in which the conduction distance, and CVN distribution were fixed), deconvolution gave precise estimates of the simulated CB, whereas area and amplitude method were affected by a positive bias, due to temporal dispersion. The effect of temporal dispersion due to a variable conduction distance was then assessed on simulated signals. Area and amplitude methods gave estimates of CB which increased with increasing temporal dispersion, whereas the deconvolution method is stable, proving that this method has limited sensitivity to temporal dispersion both in the case of phenomenological and simulated signals, obtained with an accurate surface EMG generation model.

### 4.2 Discussion of tests performed on healthy subjects

The method was finally tested on experimental signals. As observed in Olney et al., 1987, a larger temporal dispersion induced experimentally by increasing the conduction distance determines a larger bias in CB estimation by classical methods. Deconvolution showed good stability to temporal dispersion also on this set of experimental signals.

The performance of the deconvolution method proved to be better than that of either area or amplitude based methods when applied to experimental signals obtained from healthy subjects with different temporal dispersion induced by a different conduction distance between stimulation sites. Temporal dispersion is very high for pathologic subjects affected by demyelination (or impaired myelinic conduction), as a consequence of the pronounced reduction in CVN. It is then expected that the performance of deconvolution method versus area and amplitude methods can be even more evident than that presented here, in the case of pathologies with high temporal dispersion. Axonal damage and possible collateral reinnervation, inducing polyphasic MUAPs, is associated to signals that do not satisfy the hypotheses of the method. For example, the phase cancellation due to polyphasia cannot be

estimated by the method. Thus, we can expect that the performance of the method depends on the considered pathology.

### 4.3 Conclusions

A new method for the estimation of nerve CB is proposed. The method is promising for the low sensitivity to temporal dispersion of the MUAPs within the CMAP. The signals for the validation of the method were equivalent to those adopted in the classical papers Rhee et al., 1990 (for simulated signals) and Olney et al., 1987 (for experimental signals), which influenced the definition of criteria for CB identification. Under these conditions we conclude that the detrimental effect of temporal dispersion (and the consequent phase cancellation) on CB estimation from motor response can be overcome by the application of the new method proposed, based on deconvolution.

Further testing of the method in clinical research will lead to its optimisation and to the most efficient choice of the application software, in order to reduce computation time. Computation time is now of the order of 1 minute for the implementation in Matlab, version 6.5 -The Mathworks, Natick, MA- with CPU 2.8 GHz and RAM 1 GB.

An instrument applying the algorithm described in this paper has been recently patented by Politecnico di Torino (patent number TO2006A000327). Application of the method to pathological patients is under way.

## APPENDIX

### Deconvolution

Deconvolution is an inverse problem (Schoonhoven and Stegeman, 1991). Inverse problems are in general ill-posed, which means, for the problem at hand, that the solution is very sensitive to noise, to perturbations of the data, and to the approximations introduced in the

model (2). Tikhonov regularisation method (Pascual-Marqui, 1999; Tikhonov and Arsenin, 1977) was used to stabilise deconvolution. In the case in which the kernel $K(t)$ is known, the solution $\hat{x}(t)$ can be estimated by minimising, in the least square sense, the error in the reconstruction of the data (referred to as *residual norm*), with the introduction of a penalty term of the estimated solution

$$\hat{x} = \arg\min_{X} \left\{ \underbrace{\left\| v(t) - K(t) * X(t) \right\|_2^2}_{residual\ \ norm} + \alpha \underbrace{\left\| X(t) \right\|^2}_{solution\ \ norm} \right\} \tag{7}$$

where $\alpha$ is the (positive) regularisation parameter, $\|\cdot\|_2$ is the $L_2$ norm, and $\|\cdot\|$ is a Hilbert norm of the estimated solution $\hat{x}(t)$ (referred to as *solution norm*), defining the penalisation quantity. The sum of the $L_2$ norm of the estimated solution (i.e., the energy) and of its first derivative was used as solution norm

$$\left\| X(t) \right\|^2 = \left\| X(t) \right\|_2^2 + \left\| \frac{dX(t)}{dt} \right\|_2^2 . \tag{8}$$

This regularisation term requires the estimated delay distribution to be bound and smooth.

The minimisation problem (7) was solved numerically. Considering M samples, the kernel is a $M \times M$ triangular Toeplitz matrix (discrete version of the convolution operator)

$$\underline{K} = \begin{bmatrix} k_1 & 0 & \cdots & 0 \\ k_2 & k_1 & \ddots & \vdots \\ \vdots & \vdots & \ddots & 0 \\ k_M & \cdots & k_2 & k_1 \end{bmatrix} \tag{9}$$

where $k_i$ , $i=1,\ldots,M$, indicates the i$^{th}$ sample of the kernel. The CMAP $v(t)$ is sampled, so that an $M$-dimensional vector $\vec{V}$ is considered. The estimated solution $\hat{x}(t)$ is an $M$-dimensional vector. The solution of the minimisation problem (7) is given by

$$\hat{x} = (\underline{\underline{K}}^T \underline{\underline{K}} + \alpha(\underline{\underline{I}} + \underline{\underline{F}}^T \underline{\underline{F}}))^{-1} \underline{\underline{K}}^T \vec{V} \tag{10}$$

where the matrix $\underline{\underline{F}}$ is the discrete version of the first derivative operator $\underline{\underline{F}} = \begin{bmatrix} -1 & 1 & 0 & \cdots & 0 \\ 0 & -1 & 1 & \ddots & \vdots \\ \vdots & \ddots & \ddots & \ddots & \vdots \\ 0 & \cdots & 0 & -1 & 1 \end{bmatrix}$ with size $(M-1)\times M$.

The choice of the regularisation parameter $\alpha$ should take into account the trade-off between the degree of regularity of the solution and its fit to the data, reflecting an approximation error and a data noise error (Tu et al., 1997). Methods to select the regularisation parameters are the followings: discrepancy, minimum risk, ordinary cross validation, generalised cross validation, L-curve (Pascual-Marqui, 1999). For simplicity, we fixed the value $\alpha = 10^{-2} \cdot \lambda_{\max}(\underline{\underline{K}}^T \underline{\underline{K}})$, where $\lambda_{\max}(\underline{\underline{K}}^T \underline{\underline{K}})$ is the maximum eigenvalue of the matrix $\underline{\underline{K}}^T \underline{\underline{K}}$. With this choice, the maximum condition number of the matrix to be inverted in Eq. (10) is 100.

Some physiological constraints were imposed to the solution. The delay distribution $\hat{x}(t)$ was imposed to be a non-negative function with support corresponding to physiological value of CVN (which were restricted between a minimal and a maximal value $[CVN_{\min}, CVN_{\max}]$, to be chosen on the basis of the CMAPs to be processed). A projected Landweber method (Johansson et al., 2004) was implemented to impose the physiological constraints. The solution is updated in the direction of steepest descent of the square error functional $\left\| \underline{\underline{K}}\hat{x} - \vec{V} \right\|_2^2$. Then, the result is projected onto the constraint set. The algorithm is the following

$$\begin{cases} Initialisation: x_0 \\ y_{k+1} = x_k - \chi \underline{\underline{K}}^T (\underline{\underline{K}} x_k - \vec{V}), \quad \chi = \dfrac{0.9}{\lambda_{\max}(\underline{\underline{K}}^T \underline{\underline{K}})} \\ x_{k+1} = \max(y_{k+1}, 0), \qquad x_{k+1}(\bar{S}) = 0 \end{cases} \tag{11}$$

where the initialisation for $x_0$ is given by Tikhonov method, the step size parameter $\chi$ was chosen in order to achieve convergence in about 10 steps, the maximum operator in the definition of $x_{k+1}$ is evaluated component-wise (Johansson et al., 2004), and $\bar{S}$ indicates the complement to the constrained support of the solution (i.e., the support is constrained to the interval $\left[\frac{d}{CVN_{\max}}, \frac{d}{CVN_{\min}}\right]$, where $d$ is the distance from the stimulation site to the motor point).

**Estimation of the kernel**

In Eq. (2) and (7) the kernel is not known a-priori. A deconvolution method for estimating the distribution of the conduction velocity of peripheral nerve fibres was suggested in Tu et al., 1997, in the case of two compound action potentials (CAP – see also the review paper Schoonhoven and Stegeman, 1991). The kernel was evaluated by an iterative method which exploited the relation between the delay distributions for the two stimulation sites (making the assumption that the CVN is constant along the nerve and that CB is absent). Furthermore, the theoretical connection between the conduction velocity of an axon and the amplitude of the detected action potential was used.

For the problem at hand, the delay distributions of the two recorded CMAPs are affected by both the propagation along the nerve and that along the muscle (see Section 2.1). The recorded CMAPs could be affected by CB. Furthermore, there is not a precise relation between CVN and MUAP amplitude, as it depends on MU location. For these reasons, the method introduced by Tu et al., 1997 (and also other methods proposed for CAP deconvolution, Schoonhoven and Stegeman, 1991), is not feasible for the problem at hand.

The kernel must be estimated blindly (blind deconvolution). The only a-priori information on the kernel is related to its physical meaning, i.e. we know that it should have the shape of an action potential (detected by a single differential system).

For the estimation of the kernel an iterative optimisation method was chosen. The optimisation method was based on the minimisation of the sum of the residual norms (mean square error in reconstructing the measures)

$$MSE[K] = \left\| v^{dist}(t) - K(t) * x^{dist}(t) \right\|_2^2 + \left\| v^{prox}(t) - K(t) * x^{prox}(t) \right\|_2^2 \tag{12}$$

of the two CMAPs $v^{dist}(t)$ (CMAP related to the distal stimulation site) and $v^{prox}(t)$ (CMAP related to the proximal stimulation site), where $x^{dist}(t)$ and $x^{prox}(t)$ are the delay distributions correspondent to the distal and proximal CMAP, respectively.

The kernel is a representative MUAP to be convolved with the estimated delay distribution to approximate the recorded CMAPs. A MUAP can be well approximated by the associate Hermite functions (Lo Conte et al., 1994). The kernel was then expressed as a linear combination of the first six associate Hermite functions (using seven or eight functions did not improve the performances of the method)

$$K(t) \cong \sum_{n=0}^{5} \beta_{\lambda,n} u_{\lambda,n}(t) \tag{13}$$

where

$$u_{\lambda,n}(t) = \frac{1}{\sqrt{2^n n!}} H_n\left(\frac{t}{\lambda}\right) \frac{1}{\sqrt{\sqrt{\pi}\lambda}} e^{-\frac{t^2}{2\lambda^2}} \tag{14}$$

is an orthonormal basis of $L_2$, $H_n$ being the Hermite polynomials. The six considered $\beta_{\lambda,n}$ coefficients and the scaling factor $\lambda$ are the seven parameters (indicated by $\vec{p}$) determining the kernel. The optimisation was obtained with an initial kernel $K_0(t)$ which is an approximation of the distal CMAP (which is less affected by temporal dispersion) and

updating the parameters $\vec{p}$ (defining successive estimations of the kernel $K_i(t)$) in the direction opposite to that of the gradient of MSE, given by Eq. (12)

$$\vec{p}_{i+1} = \vec{p}_i - \mu \frac{\nabla MSE}{\left\| \nabla MSE \right\|_2} \ . \tag{15}$$

The parameter $\mu$ should be chosen as a trade-off between convergence rate and stability. Good performances were obtained by estimating at each step the minimum of MSE in the direction of the gradient (four step dicotomic search of the value of $\mu$, starting from $\mu = 0.25$). The parameters were updated by rule (15) till the following condition was satisfied

$$E = \frac{\sqrt{MSE[K]}}{\sqrt{\left\| v^{dist}(t) \right\|_2^2 + \left\| v^{prox}(t) \right\|_2^2}} < 8\% \ , \tag{16}$$

(referring to E as the reconstruction error) or for a maximum of ten iterations.

If the method did not reach a good reconstruction precision within ten iterations, the approximation of the kernel as given in Eq. (13) is not sufficient, and a further optimisation procedure is needed. Such a further optimisation uses the last estimated kernel $K_{10}(t)$ as the initial estimate of the kernel. The support of such an initial kernel was defined as the region in which its amplitude was larger than the 2% of its range. A slight variation of the samples of the kernel in the support so defined was introduced, with the attempt of reducing the reconstruction error. The kernel was updated along the gradient of MSE, till the limit E<8% was reached or for a maximum of five iterations.

In summary, a first method, based on the representation of the kernel as in Eq. (13), is used to obtain quickly a good approximation of the kernel, with a shape similar to that of a MUAP. A second optimisation method (based on changing slightly each of the samples of the estimated kernel within the support) is used in the case the first method did not provide the required precision in reconstructing the recorded CMAPs (Figure 6).

We can note that a 10% reconstruction error E corresponds to 20 dB SNR. In surface EMG signals, the SNR is of the order of 20 dB. This means that, in an ideal case, when E=10% the reconstruction error is only due to the noise content of the processed signal. Nevertheless, it should be noted that the reconstruction error can be due also to the activity of MUs which the method was not able to detect. For this reason, an uncertainty in CB estimation of the order of E must be considered.

## REFERENCES


Ad Hoc subcommittee of the American Academy of Neurology AIDS Task Force.Research criteria for diagnosis of chronic inflammatory demyelinating polyneuropathy (CIDP). Neurology 1991; 41: 617-618.

Enoka RM, Fuglevand AJ. Motor unit physiology: some unresolved issues. Muscle Nerve 2001; 24: 4-17, Review.

Farina D, Merletti R. A novel approach for precise simulation of the EMG signal detected by surface electrodes. IEEE Trans on Biomed Eng 2001; 48: 637-646.

Feasby TE, Brown WF, Gilbert JJ, Hahn AF. The pathological basis of conduction block in human neuropathies. J Neurol Neurosurg Psychiatry 1985; 48: 239-244.

Gazzoni M, Farina D, Merletti R. A new method for the extraction and classification of single motor unit action potentials from surface EMG signals. J Neurosci Methods 2004; 136: 165-177.

Johansson B, Elfving T, Kozlov V, Censor Y, Granlund G. The Application of an Oblique-Projected Landweber Method to a Model of Supervised Learning. 2004; LiTH-ISY-R-2623.

Kimura J. Electrodiagnosis in disease of the nerve and muscle: principles and practice.2nd ed. Philadelphia: FA Davis, pp. 103-138, 1989.

Kimura J. Consequences of peripheral nerve demyelination: basic and clinical aspects. Can J Neurol Sci 1993; 20: 263-270. Review.

Lo Conte LR, Merletti R, Sandri GV. Hermite expansions of compact support waveforms: applications to myoelectric signals. IEEE Trans on Biomed Eng 1994; 41: 1147-1159.

Mesin L, Tizzani F, Farina D. Estimation of Muscle Fiber Conduction Velocity from Surface EMG Recordings by Optimal Spatial Filtering. IEEE Trans on Biomed Eng 2006; in press.

Oh SJ, Kim DE, Kuruoglu HR. What is the best diagnostic index of conduction block and temporal dispersion? Muscle Nerve 1994; 17: 489-493.

Olney RK, Budingen HJ, Miller RG. The effect of temporal dispersion on compound action potential area in human peripheral nerve. Muscle Nerve 1987; 10:728-33.

Pascual-Marqui RD. Review of Methods for Solving the EEG Inverse Problem. International Journal of Bioelectromagnetism 1999; 1: 75-86.

Reutskiy S, Rossoni E, Tirozzi B. Conduction in bundles of demyelinated nerve fibers: computer simulation. Biol Cybern 2003; 89: 439-448.

Rhee EK, England JD, Sumner AJ. A computer simulation of conduction block: effects produced by actual block versus interphase cancellation. Ann Neurol 1990; 28: 146-156.

Rosenfalck P. Intra and extracellular fields of active nerve and muscle fibers. A physico-mathematical analysis of different models. Acta Physiol Scand 1969; 321: 1-49.

Schoonhoven R, Stegeman DF. Models and analysis of compound nerve action potentials. Crit Rev Biomed Eng. 1991; 19(1): 47-111.

Schulte-Mattler WJ, Jakob M, Zierz S. Assessment of temporal dispersion in motor nerves with normal conduction velocity. Clin Neurophysiol 1999; 110: 740-747.

Schulte-Mattler WJ, Muller T, Georgiadis D, Kornhuber ME, Zierz S. Length dependence of variables associated with temporal dispersion in human motor nerves. Muscle Nerve 2001; 24: 527-533.

Stalberg E, Karlsson L. The motor nerve simulator. Clin Neurophysiol 2001; 112: 2118-2132.

Tani T, Ushida T, Yamamoto H, Okuhara Y. Waveform changes due to conduction block and their underlying mechanism in spinal somatosensory evoked potential: a computer simulation. J Neurosurg 1997; 86: 303-310. Technical note.

Tikhonov AN, Arsenin V. Solution of Ill-Posed Problems. Wiley, New York, 1977.

Tu YX, Wernsdorfer A, Honda S, Tomita Y. Estimation of conduction velocity distribution by regularized-least-squares method. IEEE Trans on Biomed Eng 1997; 44: 1102-1106.

Troni W, Cantello R, Rainero I. Conduction velocity along human muscle fibers in situ.

Neurology 1983; 33: 1453-1459.

Van Asseldonk JT, Van den Berg LH, Wieneke GH, Wokke JH, Franssen H. Criteria for conduction block based on computer simulation studies of nerve conduction with human data obtained in the forearm segment of the median nerve. Brain. 2006; 129: 2447-60.

**FIGURE CAPTIONS**

**Fig. 1** Description of A) phenomenological and B) simulated signals. A) Phenomenological signals are obtained by a convolution, i.e. summing delayed and amplitude scaled versions of a kernel function. The delays were normally distributed, the amplitudes exponentially. An ambiguity of the number of single contributions and the amplitude of each contributions is present. B) The simulated signals were obtained by using a plane layer model to simulate single MUAPs, and by delaying such MUAPs by the calculated delay of propagation of the action potential along the nerve from the stimulation site to the end-plate.

**Fig. 2** Simulated and estimated CB using phenomenological signals. No CB was simulated. The signals were obtained by convolving the representative MUAP B) (obtained by averaging 10 decomposed single MUAPs from abductor pollicis muscle) with the delay distribution obtained given the conduction distance and the CVN distribution A). Different conduction distances and innervation ratios R were considered C), D), E). The proposed method based on deconvolution C) is compared to classical methods for CB estimation based on measures of area D) and amplitude E).

**Fig. 3** CB estimation from simulated signals, in the case of Gaussian CVN distribution centred at 47.3 m/s and with standard deviation 5.2 m/s. The distance from proximal (distal) stimulation site to the innervation zone is 320 mm (70 mm). An example of simulated and reconstructed distal and proximal CMAPs, optimal estimated kernel and estimated delay

distributions is shown in A). The proposed method based on deconvolution is compared to classical methods for CB estimation based on measures of area and amplitude in B), showing the average value and standard deviation of the estimates over 25 realisations (corresponding to 5 different distributions of the MUs in the simulated muscle, each with 5 realisations of additive Gaussian noise with SNR 20 dB).

**Fig. 4** CB estimation from simulated signals, in the case of Gaussian CVN distribution centred at 47.3 m/s and with standard deviation 5.2 m/s. Increasing temporal dispersion is simulated by increasing the conduction distance. Two examples of simulated and reconstructed distal and proximal CMAPs (correspondent to two conduction distances), optimal estimated kernel and estimated delay distributions are shown in A) and B). The proposed method based on deconvolution is compared to classical methods for CB estimation based on measures of area and amplitude in C), for two conduction distances, showing the average value and standard deviation of the estimates over 25 realisations (corresponding to 5 different distributions of the MUs in the simulated muscle, each with 5 realisations of additive Gaussian noise with SNR 20 dB). The effect of increasing the conduction distance is shown in D), for conduction distances from 150 to 350 mm.

**Fig. 5** Application of deconvolution, area and amplitude methods to experimental signals from abductor digiti minimi. Different temporal dispersions were obtained by comparing stimulation above-elbow with below-elbow (conduction distance about 100 mm) and above-elbow with wrist (conduction distance about 350 mm). Representative examples (relative to the first subject) of reconstruction of distal and proximal CMAPs (correspondent to two conduction distances), showing the optimal estimated kernel and the estimated delay distributions, are shown in A) and B). The CB estimated with the three methods for all considered 8 subjects are shown in C). The averages and standard deviations of such estimates for each method are shown in D).

**Fig. 6** Block diagram of the proposed method.

## Fig. 1

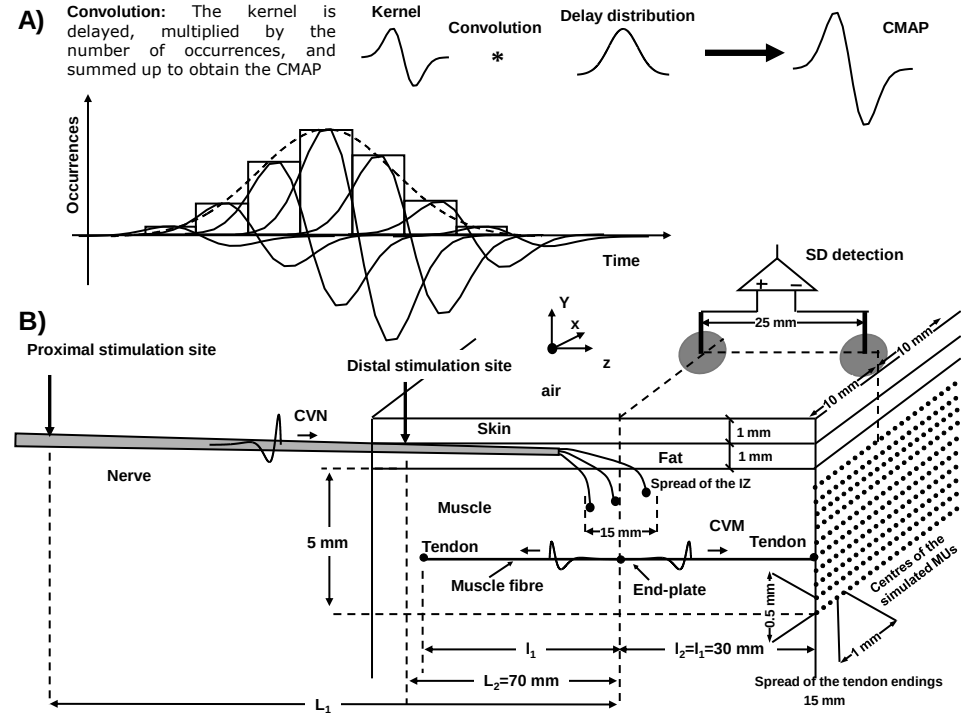


## Fig. 2

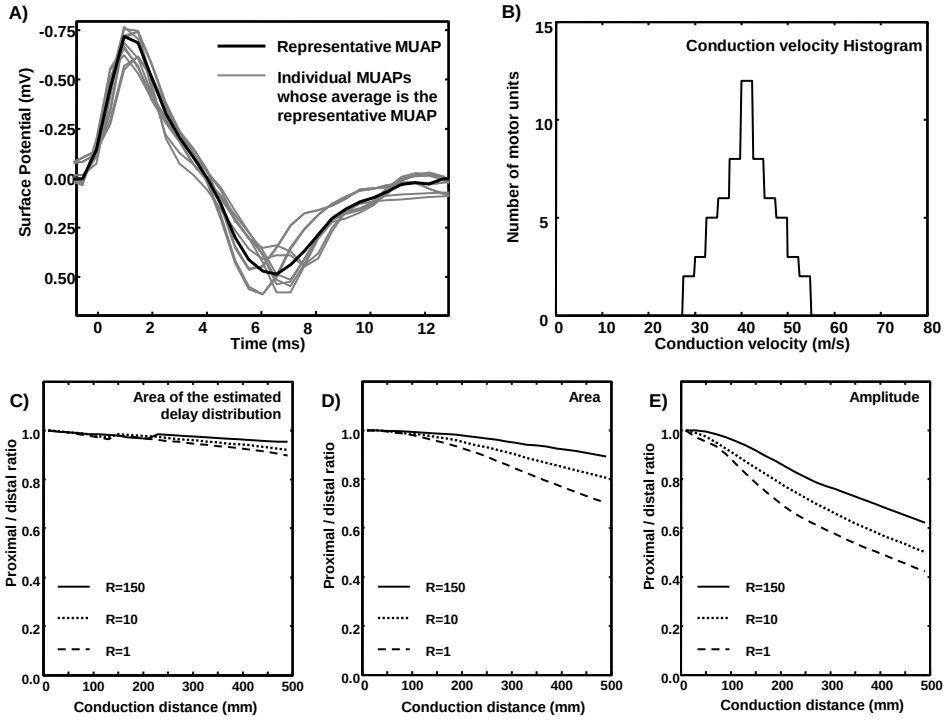

## Fig. 3

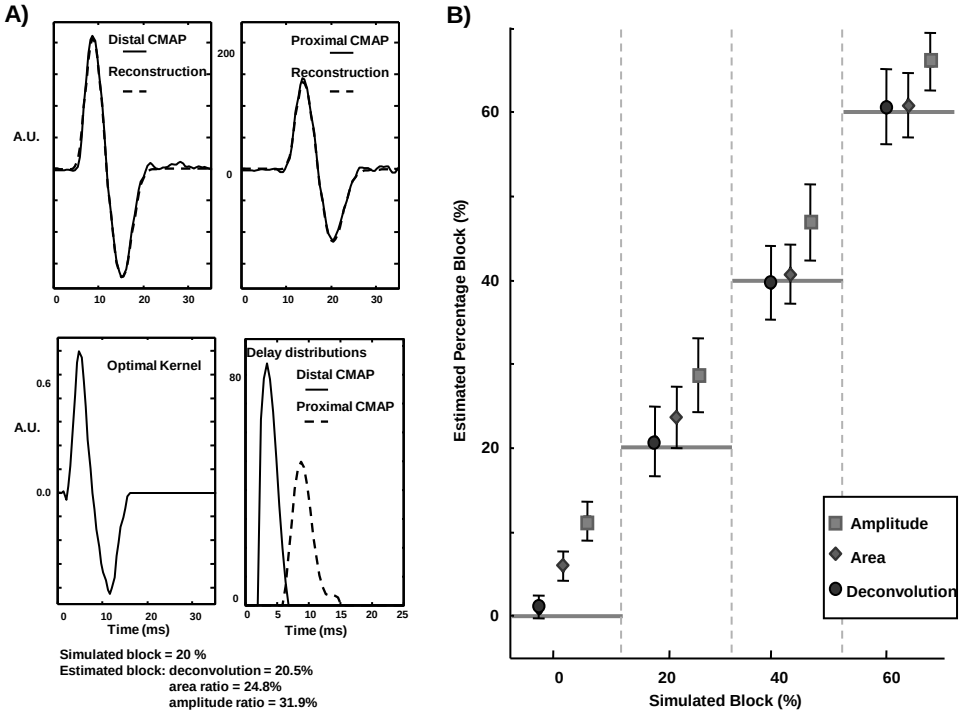
A)
Distal CMAP
Reconstruction
Proximal CMAP
Reconstruction
A.U.
Optimal Kernel
Delay distributions
Distal CMAP
Proximal CMAP
Time (ms)
Time (ms)
Simulated block = 20 %
Estimated block: deconvolution = 20.5%
area ratio = 24.8%
amplitude ratio = 31.9%
B)
Estimated Percentage Block (%)
Simulated Block (%)
Amplitude
Area
Deconvolution

## Fig. 4

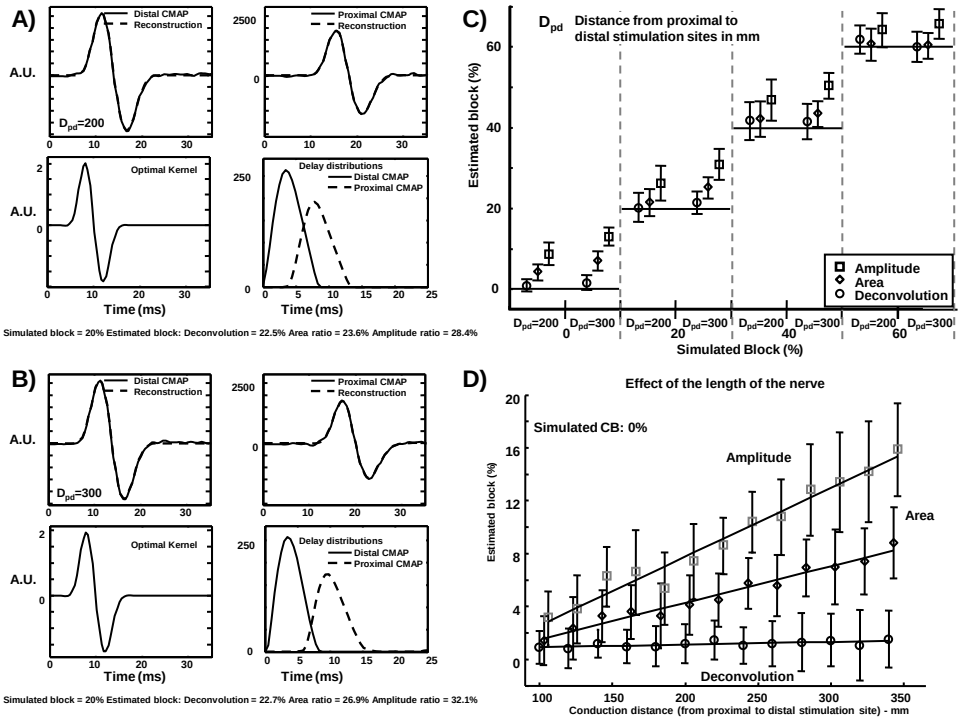
A)
Distal CMAP
Reconstruction
Proximal CMAP
Reconstruction
A.U.
Optimal Kernel
Delay distributions
Distal CMAP
Proximal CMAP
Time (ms)
Time (ms)
Simulated block = 20% Estimated block: Deconvolution = 22.5% Area ratio = 23.6% Amplitude ratio = 28.4%
B)
Distal CMAP
Reconstruction
Proximal CMAP
Reconstruction
A.U.
Optimal Kernel
Delay distributions
Distal CMAP
Proximal CMAP
Time (ms)
Time (ms)
Simulated block = 20% Estimated block: Deconvolution = 22.7% Area ratio = 26.9% Amplitude ratio = 32.1%
C)
Dpd Distance from proximal to distal stimulation sites in mm
Estimated block (%)
Amplitude
Area
Deconvolution
Simulated Block (%)
D)
Effect of the length of the nerve
Simulated CB: 0%
Amplitude
Area
Deconvolution
Estimated block (%)
Conduction distance (from proximal to distal stimulation site) - mm

## Fig. 5

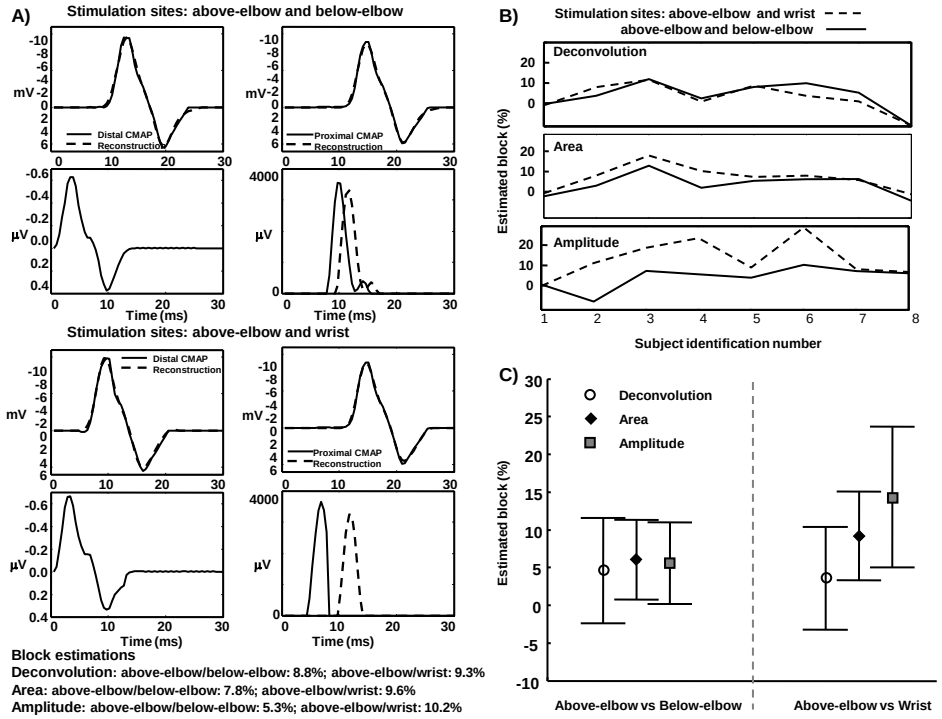
A)
Stimulation sites: above-elbow and below-elbow
Distal CMAP
Reconstruction
Proximal CMAP
Reconstruction
mV
μV
Time (ms)
Stimulation sites: above-elbow and wrist
Distal CMAP
Reconstruction
Proximal CMAP
Reconstruction
B)
Stimulation sites: above-elbow and wrist
above-elbow and below-elbow
Deconvolution
Area
Amplitude
Estimated block (%)
Subject identification number
C)
Deconvolution
Area
Amplitude
Estimated block (%)
Above-elbow vs Below-elbow
Above-elbow vs Wrist
Block estimations
Deconvolution: above-elbow/below-elbow: 8.8%; above-elbow/wrist: 9.3%
Area: above-elbow/below-elbow: 7.8%; above-elbow/wrist: 9.6%
Amplitude: above-elbow/below-elbow: 5.3%; above-elbow/wrist: 10.2%

## Fig. 6

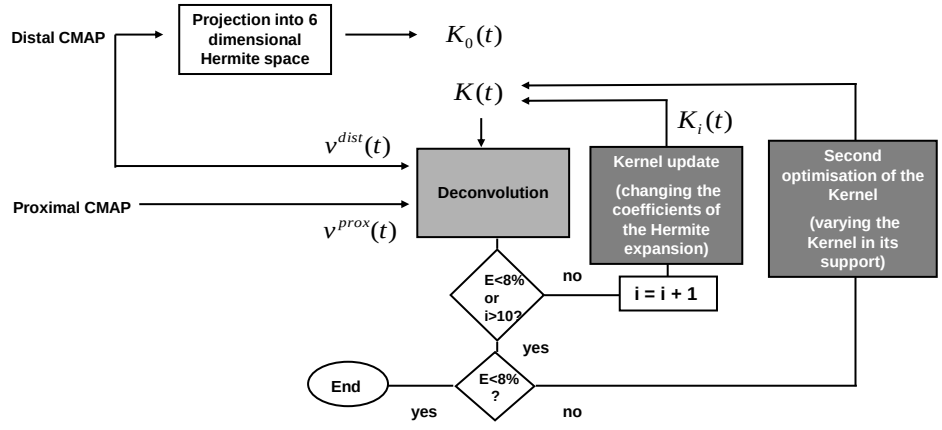
Distal CMAP
Projection into 6 dimensional Hermite space
$K_0(t)$
$K(t)$
$K_i(t)$
$v^{dist}(t)$
Proximal CMAP
$v^{prox}(t)$
Deconvolution
Kernel update
(changing the coefficients of the Hermite expansion)
Second optimisation of the Kernel
(varying the Kernel in its support)
E<8% or i>10?
no
i = i + 1
yes
End
E<8% ?
yes
no